Cellulose micro/nanocrystals reinforced polyurethane

N.E. Marcovich
Instituto de Investigaciones en Ciencia y Technologia de Materiales (INTEMA), Chemical Engineering Department, Universidad Nacional de Mar del Plata, 7600 Mar del Plata, Argentina

M.L. Auad
University of Southern California, Gill Foundation Composites Center, Los Angeles, California 90089-0241

N.E. Bellesi
Instituto de Investigaciones en Ciencia y Technologia de Materiales (INTEMA), Chemical Engineering Department, Universidad Nacional de Mar del Plata, 7600 Mar del Plata, Argentina

S.R. Nutt
University of Southern California, Gill Foundation Composites Center, Los Angeles, California 90089-0241

M.I. Aranguren[a)]
Instituto de Investigaciones en Ciencia y Technologia de Materiales (INTEMA), Chemical Engineering Department, Universidad Nacional de Mar del Plata, 7600 Mar del Plata, Argentina

(Received 14 September 2005; accepted 12 December 2005)

Nano- and micron-sized cellulose crystals were prepared and utilized as reinforcements for polyurethane composites. The cellulose crystals obtained from microcrystalline cellulose (MCC) were incorporated into a polar organic solvent, dimethylformamide (DMF), and ultrasonicated to obtain a stable suspension. The suspension was an effective means for incorporating the cellulose crystals into the polyol-isocyanate mixture, utilized to produce polyurethane composite films. The use of DMF presents an interesting alternative for the use of cellulose crystals as reinforcement of a broad new range of polymers. Moreover, the rheology of the uncured liquid suspensions was investigated, and analysis of the results indicated the formation of a filler structure pervading the liquid suspension. Besides, films were prepared by casting and thermal curing of the stable suspensions. Thermomechanical and mechanical testing of the films were carried out to analyze the performance of the composites. The results indicated that a strong filler-matrix interaction was developed during curing as a result of a chemical reaction occurring between the crystals and the isocyanate component.

I. INTRODUCTION

The combination of discrete materials has been used for decades to obtain composite materials with properties superior to either individual component. In particular, considerable effort has been devoted in recent years to the research and development of materials that utilize cellulose fibers as the load bearing constituents for different polymeric composites.[1]

Cellulose is one of the most abundant materials in nature, since it represents the main structural component of the plants and is also produced on a much smaller scale by some sea animals.[2] In addition, attributes such as low cost, low density, high stiffness, renewable nature, and biodegradability[3–6] constitute major incentives for exploring new uses. Cellulose fibers exhibit a unique structural hierarchy derived from its biological origin. They are composed of assemblies of microfibrils,[7–10] which form slender and nearly endless rods. Upon exposure to strong acids, these microfibrils break down into short crystalline rods or "cellulose microcrystals." The diameter of the individual microcrystal is on the order of 5–20 nm.[11] On the other hand, the length is shorter than that of the microfibrils, ranging from few hundreds of nanometers for wood or cotton cellulose to a few microns for cellulose from animal source (tunicates).[12]

These nano/micro crystals are also very polar and attract each other by H bonding, so treatments like the acid hydrolysis mentioned above are used in separating the individual crystals. Depending on the efficiency of these treatments, some association may remain as has been

[a)]Address all correspondence to this author.
e-mail: marangur@fi.mdp.edu.ar
DOI: 10.1557/JMR.2006.0105

shown by some other authors.[11] The strength of hydrogen bonding forces in unmodified cellulose is best exemplified in the production of "paper," where these secondary interactions provide the basis for the mechanical strength of the material.[13]

More usually, a negative surface charge is induced during the preparation of the individual cellulose microcrystals, which allows their dispersion in water.[11,13,14] Thus, a common option to prepare cellulose crystals filled polymers has been to disperse both components (matrix and filler) in water. Reports in the scientific literature have dealt with the preparation and characterization of colloidal aqueous suspensions of cellulose[14,15–17] and with the mixing of these crystals suspensions with latex[18–20] or water soluble polymers, such as starch[13,21,22] and poly(oxyethylene) (POE).[23–25] More recently, new efforts have been directed to the chemical modification of cellulose[26] and to the use of surfactants as stabilizing agents[12] with the aim of obtaining cellulose dispersions in organic nonpolar solvents and further incorporation into new polymeric matrices.

The aim of the present work was to produce a stable suspension of cellulose crystals in an organic polar solvent, dimethylformamide (DMF), to be subsequently incorporated into a polyurethane formulation to finally form crosslinked composite films. In this study, the rheological behavior of the cellulose filled liquid suspension was characterized. The morphology, as well as the thermal and mechanical behavior of the final crosslinked films was also investigated.

II. EXPERIMENTAL

A. Materials

Microcrystalline cellulose powder (MCC; Avicel PH-101 MCC, FMC BioPolymer, Philadelphia, PA) was selected as the source raw material for producing the cellulose crystals.

The matrix was formulated from a mixture of a polymeric diol (Alkuran, Alkanos, Argentina) with a hydroxyl value of 178 mg_{KOH}/g (determined in our laboratories using the techniques described elsewhere[27]), and a multifunctional polyol (Daltolac R251, Huntsman Polyurethanes, Salt Lake City, UT), with an OH value of 250 mg_{KOH}/g. The crosslinking agent was a 4,4′-diphenylmethane diisocyanate (MDI) multifunctional prepolymer (Rubinate 5005, Huntsman Polyurethanes) with an equivalent weight of 131 g/eq, which corresponds to a value of 32.08 NCO% content, as measured in our laboratory (catalog nominal value: 133 g/eq).

The samples were characterized before reaction, that is, when they were liquid mixtures of low viscosity and also after reaction in the form of crosslinked elastomeric films.

B. Methods and techniques

1. Preparation of cellulose crystals

The MCC was treated by acid hydrolysis in a concentrated sulfuric acid solution (64 wt% sulfuric acid in water). The ratio of MCC to acid solution was 1–8.75 g/ml. The treatment was performed at 45 °C and under strong stirring. The selection of the initial conditions was based on the work of Dong[14] and subsequently optimized for this system.

After treatment, the hydrolyzed cellulose (HC) was washed 4–5 times, separating the crystals from the solution by centrifuge (12,000 rpm, 10 min) after each washing. The final aqueous suspension was freeze-dried (lyophilized) to avoid re-agglomeration of the cellulose crystals. The dried crystals were re-dispersed by ultrasonic agitation in DMF. Sonication was repeated until complete re-dispersion took place. Sonication treatments were performed in plastic containers to avoid contamination from ions that could be released from glass containers.[14]

2. Preparation of liquid suspensions and crosslinked films

The polyol mixture was prepared using 60 wt% diol and 40 wt% multifunctional polyol. Then the DMF suspension of the cellulose crystals was added to this polyol mixture and the entire system was mechanically stirred and subsequently sonicated. Next, the solvent was allowed to evaporate completely at 70 °C until constant weight was achieved. Afterward, the MDI prepolymer was added in excess, to reach an isocyanate/OH group ratio equal to 1.3, and the system was mixed by hand. The rheological measurements were performed on these unreacted liquid suspensions.

To prepare the films, the above mixture was cast into a mold and cured for 1 h at 70 °C under mild pressure (10 MPa). Finally, the films were removed from the mold and postcured in an oven at 70 °C for 12 h.

3. Microscopy

Optical micrographs of the original microcellulose (MCC) were recorded using a Leica model EMLB microscope.

Atomic force microscopy (AFM; Nanoscope III Digital Instruments) was used to identify the individual nano/microcrystals of hydrolyzed cellulose.

Scanning electron microscopy (SEM; Cambridge 360) was used to observe the fracture surfaces of the composite films pre-chilled in liquid nitrogen. Samples were sputter-coated with gold prior to SEM observation.

4. X-ray diffraction

To determine the crystallinity of the cellulose, the powder was dispersed onto a stub and placed in an x-ray

diffractometer (Philips PW 1830, with Ni-filtered Cu K_α radiation at 40 kV and 30 mA). Samples were scanned from $2\theta = 5$ to 60° in steps of 0.02°. The peaks of the resultant spectra were deconvoluted and peak areas were determined. The degree of crystallinity was taken as the ratio of the areas under the deconvoluted crystal peaks with respect to the entire integrated area (crystal peaks plus amorphous background).

5. Rheological measurements

The rheological properties of the liquid suspensions were determined using a commercial rheometer equipped with a 200 g cm transducer (Rheometrics ARES). All experiments were performed under a continuous purge of dry nitrogen. Cone and plate geometry (diameter = 25 mm) was used to register the viscoelastic response of the suspensions. A linear viscoelastic response characterized the entire range of strain amplitudes used in this work (5 to 0.01%).

6. Thermal measurements

Differential scanning calorimetry (DSC) experiments were performed in a calorimeter (Perkin Elmer Pyris 1, Wellesley, MA) equipped with a cooling unit, operating under nitrogen atmosphere (20 ml/min). Measurements were performed at 10 °C/min.

A dynamic mechanical analyzer (Perkin Elmer DMA 7) was used to determine the thermomechanical response of specific samples. Tests were conducted using the temperature scan mode, a three point bending fixture with a 15 mm specimen platform, and dynamic and static stresses of 3×10^5 and 5×10^5 Pa, respectively. The frequency of the forced oscillations was fixed at 1 Hz. The specimens were cut to approximately $20 \times 3 \times 2$ mm^3, and the linear dimensions were measured to an accuracy of 0.01 mm. The main relaxation temperatures associated with T_g were determined from the temperature position of the maximum in tan δ.

7. Tensile tests

Microtensile specimens 5×25 mm were cut from the molded films and tested at 20 °C using a loading rate of 10 mm/min (INSTRON 8501, Norwood, MA), in accordance with ASTM D 1708. At least five replicates of each sample were measured, and the average values were reported.

III. RESULTS AND DISCUSSION

A. Characterization of the cellulose crystals

1. X-ray difraction

The crystallinity of MCC was consistent with reports in the literature.[2,28,29] The contribution of the crystalline peaks increased after acid hydrolysis. This was an expected result, because the amorphous regions of the MCC are more susceptible to acid attack. However, the diffraction patterns indicated the presence of a significant volume of remaining amorphous cellulose. The percentage of crystallinity increased from 56% to 67% after the hydrolysis, in agreement with previous reports for cellulose crystals obtained from other vegetable sources.[2,30,31]

2. Microscopy and dispersion of the cellulose crystals

The original MCC powder was examined by optical microscopy after dispersion in dimethylformamide at 0.1 wt% (Fig. 1). Large agglomerates (around to 30 μm) were observed under these conditions. These large agglomerated structures are formed by the strong hydrogen bonding between bundles of microfibrils. Large size structures like the ones seen in Fig. 1 have been observed by other researchers in MCC and are characteristic of this cellulose powder.[2]

After acidic hydrolysis, the agglomerated structures present in MCC were broken, and fibril bundles were separated, leaving shorter crystallites of cellulose. As detailed before, the aqueous suspension was freeze dried and the crystals further redispersed in DMF. Sonication was utilized to achieve the complete dispersion of the crystals and the resulting suspension remained stable for at least three days.

An aliquot of the DMF suspension was further diluted in the solvent and sonicated; the AFM study was performed on these preparations (Fig. 2). Individual crystals are observed that show diameters in the range of 10 to 15 nm, with aspect ratios from 10 to 15. These results are in agreement with reported characteristics of cellulose crystals from vegetable sources[11] but are much shorter than cellulose whiskers from animal sources.[11,32]

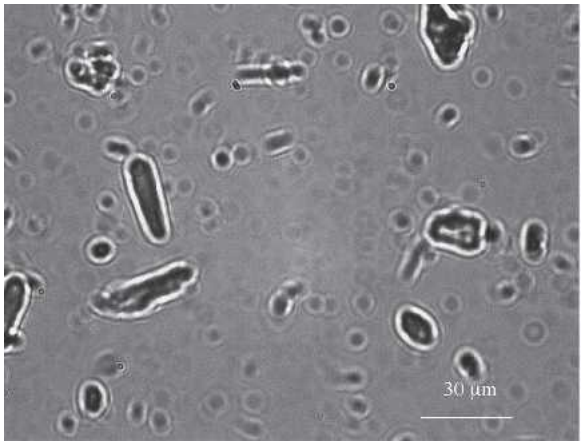

FIG. 1. Optical microscopy of microcrystalline cellulose before hydrolysis.

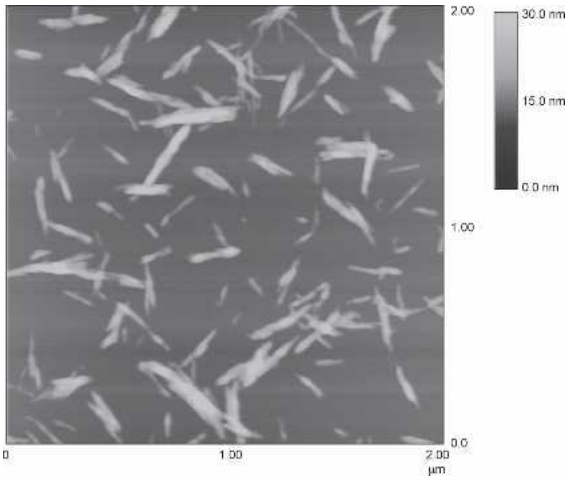

FIG. 2. Atomic force microscopy of hydrolyzed cellulose crystals.

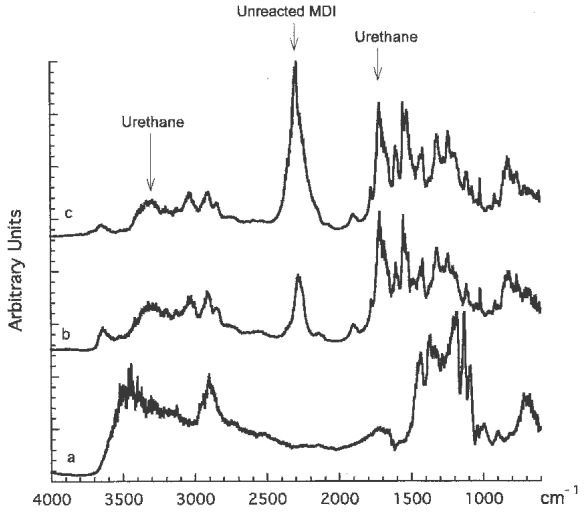

FIG. 3. FTIR spectra of hydrolized cellulose before and after reaction with MDI prepolymer: (a) hydrolyzed cellulose, (b) MDI reacted HC sample after washing it with toluene, and (c) MDI reacted HC.

Figure 2 also shows that there are still some associated crystals (bundles). This association might exist originally in the suspension or it may be the result of the drying process (DMF evaporation).

B. Filler–polymer interactions

1. Liquid suspensions of cellulose crystals

In the liquid suspensions, interfacial polar interactions are possible between the crystals and the liquid polymeric components. There are also strong H-bonding forces between the crystals themselves. The low viscosity of the liquid medium allows the cellulose crystals to move due to thermal fluctuations. The crystals can spatially rearrange, touch, and form large structures if the sample is at rest or orientate and separate if the sample is under shearing.

2. Reacted systems: Cellulose-reinforced PU films

A strong interaction matrix-reinforcement is developed during curing through a chemical reaction between the OH groups of the cellulose and the MDI-prepolymer. Isocyanate or polyurethane formulations have been used for decades as wood adhesives and coatings, so this reaction was expected. To confirm its occurrence, hydrolyzed cellulose crystals were mixed with excess MDI and heated at 70 °C (the same temperature used in curing the composite films). After curing 1 h under pressure, samples were milled and analyzed by diffuse reflectance Fourier transform infrared (DRIFT). Figure 3 shows the spectra of the hydrolyzed cellulose (curve a) and the mixture of MDI + hydrolyzed cellulose after curing (curve c). In addition to the isocyanate peak (2270 cm^{-1}), a new peak appears at 1720 cm^{-1}, corresponding to the formation of urethane. Curve b (Fig. 3) corresponds to the reacted sample after washing it with toluene (to remove unreacted MDI) and further evaporation of the solvent. The large reduction in the isocyanate absorption peak indicates that MDI was removed, although not completely (the NCO group gives a strong peak in FTIR). On the other hand, there is no reduction of the 1720 cm^{-1} peak, since urethane groups are not removed by washing and remain attached to the cellulose crystals. These observations confirm that the MDI prepolymer reacts with the cellulose.

The reduction of the peak intensity corresponding to the OH groups (3500 cm^{-1}) is particularly significant. Since the OH groups participate in the reaction to form the urethane groups, the OH absorption-peak practically disappear at the end of the reaction. This is of fundamental importance to further understand the behavior of the cured samples. Because cellulose crystals can strongly interact through H-bonding, the disappearance of the OH groups reduces direct filler–filler interaction, and this has profound effects on the final material behavior, as it will be discussed later.

C. Characterization of the unreacted liquid suspensions

The rheological characterization of the liquid suspensions made from the polyols and MDI prepolymer with and without hydrolyzed cellulose crystals is summarized in Fig. 4. The measurements were carried out in the linear viscoelastic range, using small strains. Figure 4(a) shows the dynamic viscosity of the samples plotted as a function of the frequency for different crystal concentrations. The gelation time for these samples at room temperature was longer than 2 h. Consequently, any changes in the viscosity related to the sample reaction during the frequency sweep tests can be neglected. A confirmation of this statement is given by the lower curve of Fig. 4(a), which corresponds to the neat liquid sample. As shown,

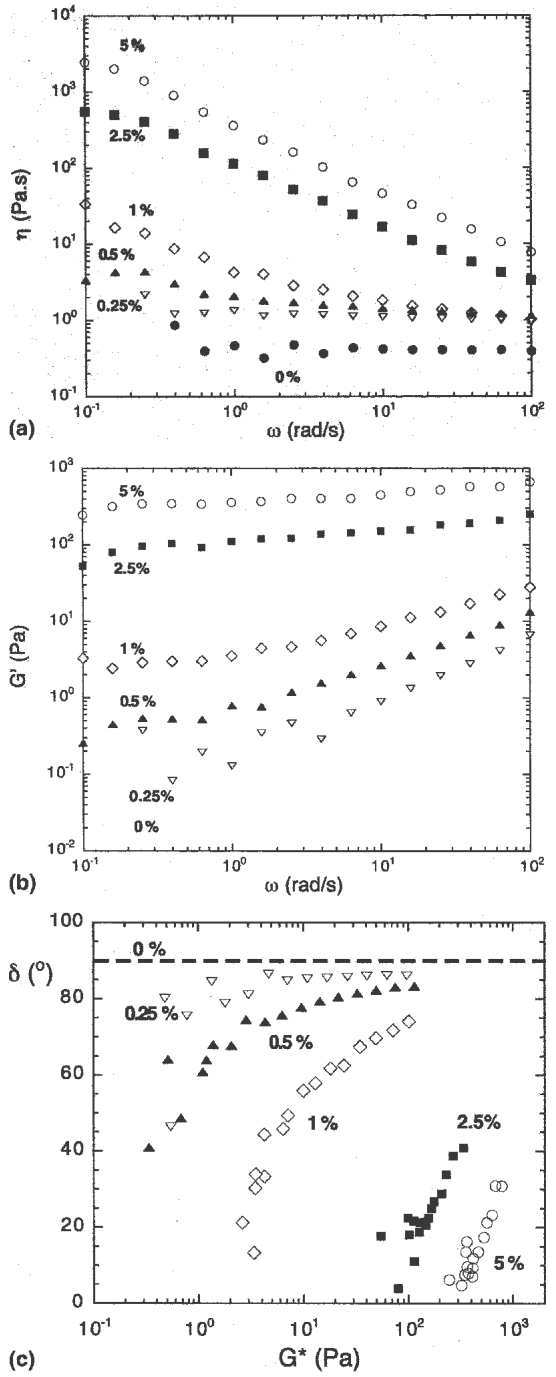

FIG. 4. Rheological behavior of unreacted liquid mixtures of the polyols and MDI prepolymer with and without hydrolyzed cellulose crystals: (a) dynamic viscosity versus frequency, (b) storage modulus (G') versus frequency, (c) Van Gurp–Palmen plot.

the sample behaves as a Newtonian liquid and the viscosity remains constant during the duration of the test.

Figure 4(a) shows that the addition of a small amount of cellulose crystals (5 wt%) was sufficient to increase the low-frequency viscosity to a value about 6100 times higher than that of the neat mixture and 20 times higher if the high frequency range is considered. This is a clear indication of the non-Newtonian behavior introduced by the presence of the crystals. At about 0.5–1 wt% cellulose concentration, the behavior of the liquid suspension presented a qualitative change as compared to the neat sample. That is, a Newtonian plateau at low frequencies and shear thinning at increasing frequencies are observed. Further addition of crystals (2.5, 5 wt%) resulted in a power law behavior that extended over the entire range of frequencies studied.

The plateau developed at intermediate concentrations (around 0.5–1 wt%) has been ascribed to the structure formed by the crystals due to interparticle interactions. These interactions present a high resistance to flow and are the reason for the frequency independence observed. At higher frequencies, the structure breaks down into individual crystals (or at least into smaller fragments). This rheological behavior is not new for particle suspensions literature.[33–35] Similar observations have been reported in the literature for years, in studies of liquid rubbers (unreacted systems) filled with carbon black or silicas. In both cases, a qualitative change was observed between 20 and 40 wt% (around 15–30% by volume).[35] Although the individual particles of these fillers may be very small (10–30 nm), they are present in the rubber as partially fused aggregates close to micron size.

Many simple models for describing the viscosity of particle suspensions have been derived from Einstein equation. They only consider the volume concentration of the particles, and their aspect ratio for the case of non-spherical particles.[36] These models take into account the hydrodynamic effects of the particles on the flow field and the result is a modest increase of viscosity with filler concentration. Some models are formulated to predict an infinite viscosity of the suspension at the maximum packing of the particles,[37] which is experimentally found to be 0.6–0.7 volume fraction for spheres (hard sphere models). Instead, if the particles have irregular forms the maximum packing is reduced, and in the case of rods with an aspect ratio of 27 the maximum packing drops to 0.18 according to Metzner.[38]

One of the equations that take into account the aspect ratio of the particles is shown below[36,39]:

$$\frac{\eta}{\eta_\infty} = 1 + 0.67\ \phi_f f + 1.62\ \phi_f^2 f^2 \quad , \qquad (1)$$

where η is the viscosity of the suspension, η_m is the viscosity of the suspending media, ϕ is the volume fraction of the particles, and f is the aspect ratio.

The results of the predicted and experimental viscosities for the suspensions (expressed as η/η_m) at low frequencies are presented in Table I. Comparison of the values shows clearly that the experimental behavior cannot be explained by the simple hydrodynamic effect of the particles in the liquid media. Even considering

TABLE I. Predicted [according to Eq. (1)] and experimental viscosities allow frequencies of hydrolyzed cellulose–liquid prepolymer suspensions.

HC wt%	0	0.25	0.5	1	2.5	5
Volumetric fraction, ϕ	0.00	0.0016	0.0033	0.0066	0.0165	0.0333
η/η_∞, experimental	1.00	5.2676	19.823	82.188	1337.7	5952.2
η/η_∞, predicted, $f = 10$	1.00	1.011	1.024	1.051	1.154	1.402
η/η_∞, predicted, $f = 20$	1.00	1.024	1.051	1.116	1.397	2.162
η/η_∞, $f = 100$	1.00	1.153	1.393	2.136	6.506	21.15

artificial aspect ratios as large as 100, the prediction is orders of magnitude below the measured value.

The actual experimental results are more consistent with a system of percolating cellulose crystals in the liquid polymer precursors. This observation is in good agreement with the findings of other authors that have worked with cellulose whiskers.[18,21]

On the other hand, the shear thinning behavior observed at high frequencies or covering the entire range of frequencies for the highly concentrated samples is the result of the alignment of the crystals under flow, as it has been described for cellulose aqueous suspensions.[11,33]

The material response can also be presented as the storage modulus of the suspension G' versus the frequency [Fig. 4(b)]. Again, the largest differences between the different curves occur in the low-frequency range. In particular, the storage modulus of the neat sample was below the resolution of the equipment, since the neat sample behaved as a Newtonian liquid. Consequently, the corresponding G' value was essentially zero. On the other hand, the storage modulus of the suspensions increased with increasing crystal concentration, while the sample containing 1 wt% crystals showed an equilibrium plateau at low frequencies. Moreover, samples containing 2.5 and 5 wt% crystals showed a behavior similar to that of a rubber of low crosslinking density, indicating that extensive contact between the crystals occurs at these concentrations. Clearly, a qualitative change occurred with increasing crystal concentration, from a Newtonian liquid to a viscoelastic liquid to a viscoelastic solid. Thus, at a frequency of 1 rad/s, a 2800-fold increment in modulus resulted from increasing crystal concentration from 0.25 to 5 wt%, indicative of the formation of a structure in the liquid, due to a pervading network of crystals.

The above results indicate that large scale relaxations in the crystal-filled suspension are restrained by the presence of cellulose particles. A filler network is formed, which interferes with long-range motions of polymer chains (polyols and MDI prepolymer).[40] At high frequencies, the effect of the filler on the rheological behavior is comparatively weaker, as it also occurred with the dynamic viscosity. This phenomenon has been observed for other polymeric filled suspensions where the short length dynamics is approximately unchanged, while the terminal behavior is strongly modified.[41]

Finally, the results can also be analyzed using a van Gurp–Palmen plot,[42] in which the phase angle δ is plotted against the complex dynamic modulus, G^* [Fig. 4(c)]. The neat sample, which exhibits Newtonian liquid behavior, is expected to be completely out of phase with respect to the sinusoidal strain input ($\delta = 90°$). For the remaining samples, viscoelastic behavior is observed, in which the phase angle is nearly 90° at high frequencies but decreases at lower frequencies. The curve corresponding to the 1 wt% suspension shows a large curvature. By a simple extrapolation of the data, a non-zero G^* value is reached at a phase angle of 0° (solid-like behavior). This kind of plot does not clearly distinguish between liquid viscoelastic and solid viscoelastic behavior, but it offers a rapid means of identifying the range of concentrations around which this change occurs.

Moreover, the experimental data for the equilibrium modulus of the filled liquid mixtures at low frequencies (unbroken crystals structure) was modeled as a function of the crystals concentration according to a percolation expression as follows[41,43,44]:

$$G' \propto (m - m_{cG'})^{\beta_G} \quad , \tag{2}$$

where m is the weight percent of crystals, m_{cG} is m at the threshold, and $\beta_{G'}$ is an exponent, and the equation can be applied only near the percolation threshold.

The experimental data measured at a low frequency (1 rad/s) were fitted to Eq. (2), leaving as adjustable

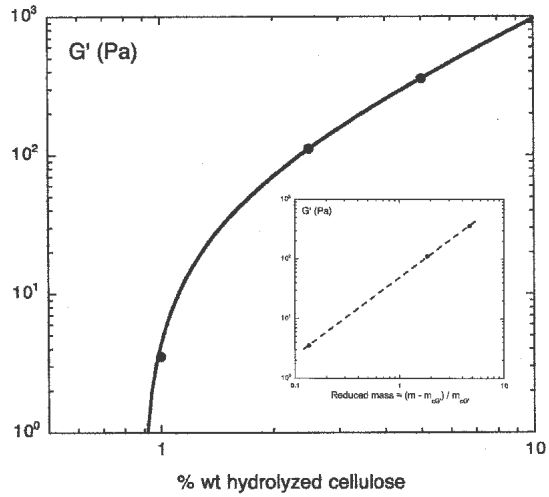

FIG. 5. Storage modulus (G') versus cellulose weight percent behavior, fitted using the percolation model [Eq. (2)].

parameters the concentration at the threshold m_{cG} and the exponent, $\beta_{G'}$. As shown in Fig. 5, the experimental data are well modeled by the equation, from which a critical concentration of 0.88 wt% is determined. The value also lies in the range of concentrations for which the qualitative change in suspension behavior was observed. The experimental data are well fitted with an exponent of 1.25 ± 0.07.[43–45]

D. Cured materials

Composite films (100 μm thickness) prepared with up to 4 wt% of cellulose crystals retained the transparency observed in the neat samples. However, all cured films acquired a yellowish hue from the use of the MDI prepolymer, which has a dark brown color.

1. Morphology of the composite films

Film samples filled with different concentrations of cellulose crystals were fractured at liquid N_2 temperature. Figure 6(a) shows that the fracture surface of the neat matrix is completely featureless, as expected for a monolithic homogeneous material. In contrast, Fig. 6(b) shows the fracture surface of a sample with 0.25 wt% of crystals, and the appearance is qualitatively different. The surface is rougher, indicating increased energy dissipation during fracture. The advancing crack must change path (deflection) because of the presence of the rigid filler material, in this case, the cellulose crystals. The higher the crystal concentration, the greater the density of crack deflection sites, producing smaller and denser ripples and ridges [Figs. 6(c)–6(e)].

The parabolic markings observed in Fig. 7(a) produced a fish-scale appearance in the composite fracture surfaces, but not in the neat sample. These features have been reported previously in cross-linked thermosets and also in linear polymers.[46–49] These types of markings appear because secondary cracks are generated in a region of high stress located in the path of the primary crack. When the velocities of the primary and secondary cracks are equal, a parabolic crack shape results. Stress concentrations occur because of the presence of "defects"

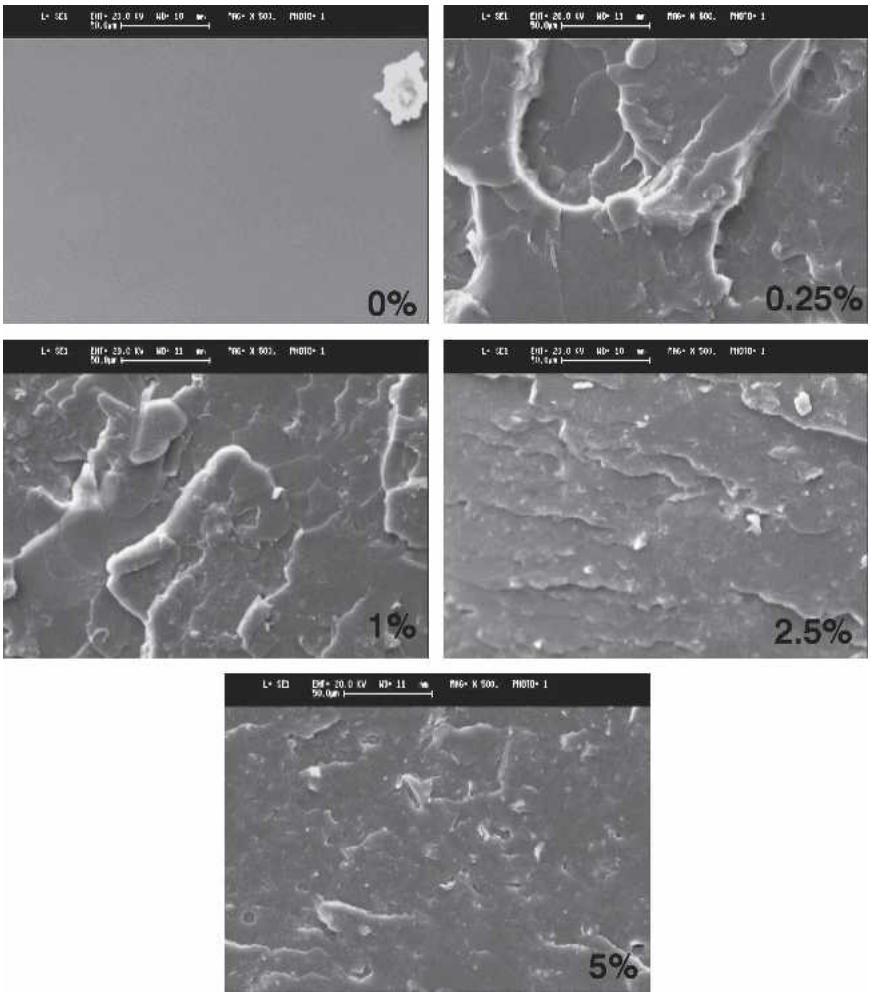

FIG. 6. Scanning electron microscopy of low temperature fractured surfaces of composites prepared with different HC content (wt%).

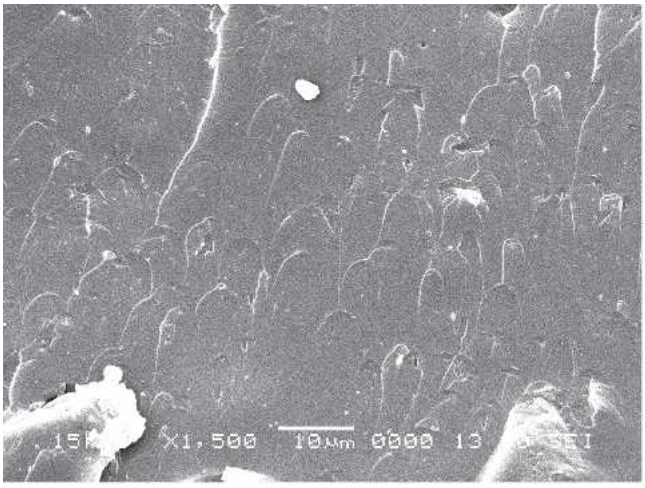

(a)

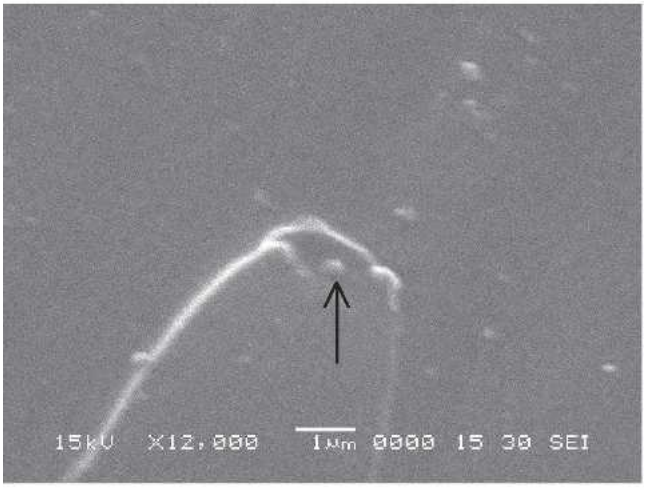

(b)

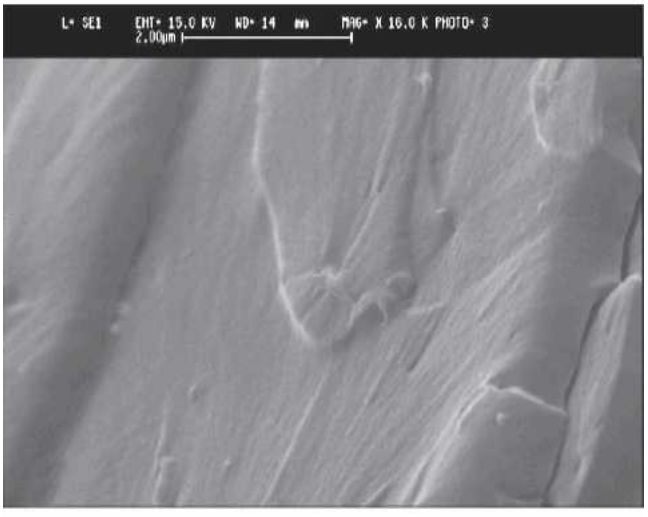

(c)

FIG. 7. Detail of parabolic markings in fractured surfaces: (a) 1500×, (b) detail, 12000×, and (c) detail from an angle.

in the material, such as entrapped gas bubbles, impurities, etc. In the present case, the number of parabolic markings increased with increasing crystal concentration. Figure 7(b) shows that near the vertex of one of these parabolic features, there is a point-like feature, assumed to be the cross-section of a crystal located in the path of the advancing crack. Figure 7(c) shows a marking from an angle, illustrating that these features are located in a different plane than the primary crack.[49] Cottrell[50] has noted rather early that the density of parabolic markings is correlated with the energy consumed and thus, with fracture toughness. This may also have a positive effect on the tearing properties of the composite elastomers.

Regarding the appearance of the crystals in the fracture surface, there has been a recent report on cryo-fractured surfaces of nanocomposites containing tunicin cellulose whiskers.[33] As in our study, the filled films appear containing white dots, which were ascribed, as in our case, to the transversal sections of the cellulose crystals. Moreover, the observation of our materials, shows that the dots in Fig. 7 appear well distributed and separated, which is a confirmation of the success in preparing composite polyurethane films by casting from DMF solution/suspension.

2. Thermomechanical characterization of the composite films

The temperature position of the main relaxation process associated with the glass–rubber transition of the polymeric matrix is denoted T_α. This temperature is related to the T_g of the matrix and to the drop of the storage modulus (in a temperature scan), known as mechanical coupling effect.[33] The α transition of the PU samples was wide, and this was direct result of the use of a polyol mixture for the production of the films. Despite this inconvenience in the analysis, it was observed that the values of T_α increased with increasing cellulose crystal concentration, from ~30 °C for the neat PU film to 46 °C for the 2.5 wt% cellulose-filled sample. This constitutes a substantial shift, a phenomenon that has not been reported in other cellulose-filled systems. Moreover, studies in which nanofillers/nanoreinforcements with high surface/volume ratio have been utilized have not produced noticeable shifts in T_g or in T_α values.[19,21]

To confirm the observed trend, plaques (3 mm thick) were prepared using only the multifunctional polyol in the formulation (the excess of isocyanate/OH groups was maintained at 1.3). DMA analysis was performed on samples under three-point bending mode. The tan δ curves obtained for the neat resin and the 5 wt% samples are shown in Fig. 8. The use of a single polyol in the formulation resulted in a narrower temperature interval for the α transition. However, the same trend was observed, i.e., the addition of only 5 wt% cellulose crystals produced a shift in the position of the tan δ peak toward

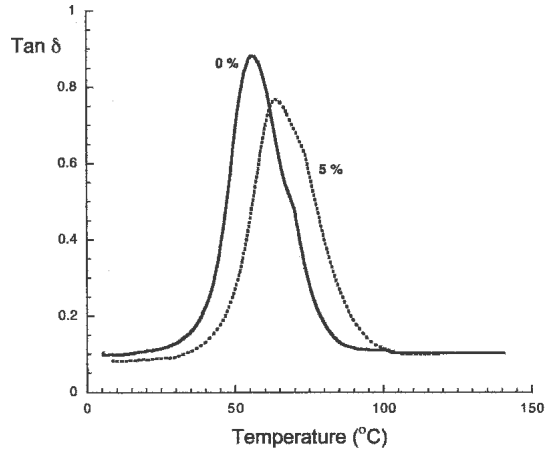

FIG. 8. Tan δ versus temperature curves obtained for the neat and the 5 wt% samples (prepared from the multifunctional polyol + MDI).

higher temperatures, from 56 °C (neat PU film) to 63.5 °C (filled film). The T_g for this formulation could be easily measured by DSC, too. Figure 9 shows the DSC thermograms corresponding to the same materials as in Fig. 8. There is an effective shift toward higher temperatures in the glass–rubber transition caused by addition of 5 wt% cellulose nanocrystals. Besides, the neat material exhibit some aging in the first DSC scan that was not apparent in the nanocomposite sample. This effect may be related to different free volume contributions and distributions in the two different samples. The effect is currently studied by positron anihilation techniques and will be the subject of future publications.

As noted above, large changes in T_g or in T_α with the addition of cellulose whiskers in different matrices have not been reported.[19,21] Evidently, the sole presence of a high surface area nano-reinforcement cannot explain the present observation. As mentioned already in the discussion of filler-polymer interactions, a reaction takes place

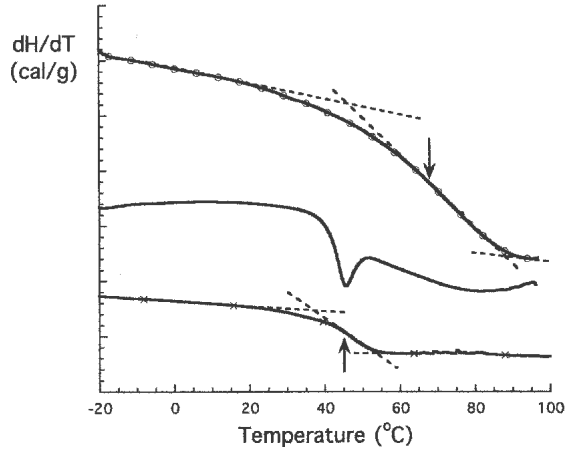

FIG. 9. DSC curves obtained from reinforced and unreinforced plaques, prepared as in Fig. 8: Neat resin, first scan (middle curve); Neat resin, second scan (lower curve); 5 wt% composite (upper curve).

TABLE II. Tensile behavior of hydrolyzed cellulose (HC)–polyurethane composites.

HC (wt%)	Tensile modulus (MPa)	Yield stress (MPa)	Deformation at yield (mm/mm)
0	41.16 ± 14.10	14.05 ± 1.39	0.55 ± 0.06
0.5	63.85 ± 3.00	11.47 ± 0.64	0.31 ± 0.03
1.0	61.99 ± 7.23	7.24 ± 0.24	0.25 ± 0.02
2.5	83.46 ± 6.52	9.98 ± 1.82	0.27 ± 0.03
5.0	100.28 ± 12.28	8.74 ± 1.16	0.26 ± 0.09

between the crystals and the MDI prepolymer, increasing the crosslinking density of the PU above the value corresponding to the unfilled PU films. The cellulose crystals act as multifunctional crosslinkers, and this reduces the mobility of the matrix and causes the large increment in T_g and the related increment in T_α.

3. Tensile behavior of the films

Films prepared from the polyol mixture and different concentrations of cellulose crystals were tested under tension. All tensile tests were performed at room temperature, that is, below the T_α of the materials. Variations due to the temperature dependence of the modulus of the materials were assumed to be negligible in the analysis of the results.

The elongation-to-failure decreased with increasing additions of cellulose crystals (Table II). Meincke et al.[42] reported similar behavior for carbon nanotube/carbon black-polyamide-6 and derivative blends, although in their case, the decrease in ductility was more dramatic. In the present study, the behavior of the filled PU remained similar to that of a hard rubber (26% ultimate strain for the 5 wt% sample).

The Young's moduli of the materials were calculated from the initial linear region of the stress–strain curves and are plotted in Fig. 10. The sample modulus increased with increasing filler content. The addition of 5 wt%

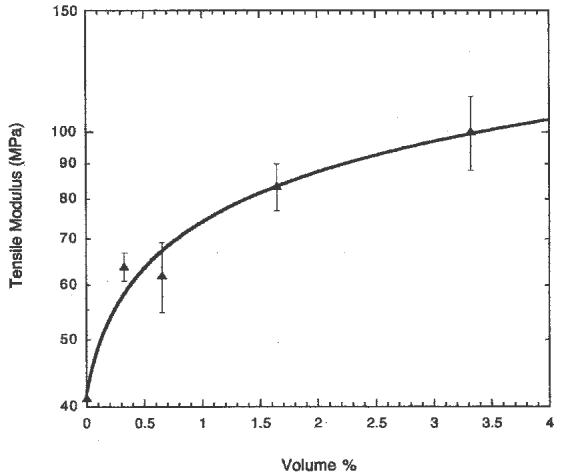

FIG. 10. Tensile modulus versus HC vol%.

cellulose nanocrystals, which corresponds to 3.5 vol%, produced a more than 2-fold increase in the Young modulus with respect to the neat system (modulus of the composite / modulus of the unfilled PU = increase factor = 2.44).

This increase in the modulus of the composites is rather modest if compared to the increase measured by other authors using cellulose whiskers, where direct contact and strong interaction between long crystals is possible. For example, Azizi Samir et al.[33] reported an increase of the tensile modulus from 0.81 to 22.3 for an unsaturated polyester thermoset with the addition of only 6 wt% cellulose whiskers (increase factor = 27.53).

On the other hand, if the improvement in tensile modulus is compared with the effect obtained in traditional composites, the increase is very large. For example, for composites prepared with a unsaturated polyester matrix filled with woodflour (a cellulosic macro filler), the flexural modulus changes from 2.9 GPa for the unfilled matrix to 5.44 GPa (increase factor = 1.8) for a relatively much higher concentration of 40 wt%.[51] Similarly, an increase factor of 1.9 in tensile modulus was measured for a polypropylene-woodflour composite also at 40 wt% of woodflour.[52]

On the other hand, some nanocomposites obtained from an unsaturated polyester and montmorillonite showed an improvement in the tensile modulus corresponding to an increase factor of only 1.18 at 3.5% volume fraction.[53] Notice that at the same volume fraction of 3.5% (5 wt%), the PU composite films corresponding to the present study show a factor increase of 2.44. The same calculation for the PU-cellulose system made at 100 °C, a temperature well above the T_g of the film, results in a increase factor of 5.65. This observation indicates that the improvement in the modulus of the composites can be ascribed to the effect of the contributed rigidity of the crystals, as well as the higher crosslinking density of the matrix.

Although simple models are available in the literature that correlate the modulus of the composites with the concentration of fillers/reinforcements,[54] none of them are directly applicable to the present system. As explained in the previous section, a reaction occurs between the bulk polyurethane and the cellulose crystals through the MDI molecules. As a result, there is an increase in the crosslinking density of the elastomer. Because the effect of this reaction depends on the cellulose concentration, each point in Fig. 10 corresponds to a material with a different matrix modulus. For this reason, a simple equation that would utilize a constant matrix modulus is unsuitable for modeling these data. On the other hand, the curve does not show a step increment at any of the prepared compositions, as expected for a percolating system. A similar response in the final solid material has been reported for systems of polyamide and carbon nanotubes or carbon black.[42] Even when extremely large increments in properties are observed,[18,19] there are no step increment with varying concentration of the fillers.

Additionally, Bréchet et al.[55] reported that the final properties in solid nanocomposites could vary strongly with the strength of the filler–filler and filler–matrix interactions. Thus, systems in which the interaction filler–filler is strong and where fillers can spatially rearrange to increase interaction exhibit percolation features. For example, when particles interacting through hydrogen bonding are immersed in a liquid suspension or in a melt, percolation behavior is observed.[6,33,34,55] In the present case, this occurs in the uncured liquid suspensions, where the crystals can rearrange spatially through a low viscosity medium, and thus a crystal structure can be formed at rest or broken accordingly to the strains and frequencies externally imposed.

In contrast, systems exhibiting a strong filler–matrix interaction show enhancements in mechanical properties, but below those predicted by percolation models and without a step increment at any filler concentration. It appears that the joints between fillers are not produced by direct contact but occur through the interaction of intermediate polymer chains, as it was already discussed. In this case, the filler structure formed consist on filler–polymer–filler connections. Naturally, the modulus of this combined structure is much lower than that of a structure formed by direct filler contacts. This is the case of the cured systems in the present work. Summarizing, the reaction between the cellulose crystals and the PU matrix reduces the direct contact and crystal–crystal interaction. Consequently, percolation behavior is not expected, nor it is observed experimentally.

IV. CONCLUSIONS

Stable suspensions of cellulose nanocrystals in DMF can be obtained, offering an alternative to the use of different polymers as potential matrices. The DMF suspensions can be successfully used in the production of PU composites that are as transparent as the neat PU.

The morphology of the filled films indicates a good dispersion of the crystals, and the effectiveness of the casting method. Cryo-fractured surfaces show that higher energy is consumed in the fracture of the composite films. It is suggested that this could result in improved tearing characteristics of these materials.

The rheology of the liquid suspensions indicated a percolation behavior at a crystal concentration threshold close to 1 wt%. The shear thinning observed at high frequencies is characteristic of filled suspensions and can be a positive feature for processing at low viscosities.

Cellulose crystals become chemically bonded to the matrix during curing, through the reaction of the OH

groups in the crystals and the isocyanate prepolymer. This reaction leads to the increase in the T_g of the PU matrix as more crystals are added.

Cellulose crystals can significantly increase the tensile modulus of the PU films at very small filler loadings (i.e., 0.5–5 wt%). Due to the strong filler–matrix reaction, there is no filler percolation in the cured films, but an increase in the crosslinking density of the PU matrix.

ACKNOWLEDGMENTS

N. E. Marcovich thanks the Science and Technology National Promotion Agency (ANPCyT) for the Grant PICT No. 14604. The authors thank the financial support of the National Research Council of Argentina (CONICET) and National University of Mar del Plata (UNMdP). M.L. Auad and S.R. Nutt gratefully acknowledge support from the Merwyn C. Gill Foundation.

Thanks are also due to Huntsman Polyurethanes for supplying the chemicals utilized in this work and to Prof. Julia Kornfield (Department of Materials Engineering, CALTECH) for the use of the ARES rheometer.

REFERENCES

1. S.J. Eichhorn, C.A. Baillie, N. Zafeiropoulos, L.Y. Mwaikambo, M.P. Ansell, A. Dufresne, K.M. Entwistle, P.J. Herrera-Franco, G.C. Escamilla, L. Groom, M. Hughes, C. Hill, T.G. Rials, and P.M. Wild: Review current international research into cellulosic fibres and composites. *J. Mater. Sci.* **36,** 2107 (2001).
2. S.J. Eichhorn and R.J. Young: The Young's modulus of a microcrystalline cellulose. *Cellulose* **8,** 197 (2001).
3. P. Zadorecki and A. Michell: Future prospects for wood cellulose as reinforcement in organic polymer composites. *Polym. Compos.* **10,** 69 (1989).
4. A. Boldizar, C. Klason, J. Kubat, P. Näslund, and P. Saha: Prehydrolyzed cellulose as reinforcing filler for thermoplastics. *Int. J. Polym. Mater.* **11,** 229 (1987).
5. R.T. Woodhams, G. Thomas, and D.K. Rogers: Wood fibers as reinforcing fillers for polyolefins. *Polym. Eng. Sci.* **24,** 1166 (1984).
6. C. Goussé, H. Chanzy, M.L. Cerrada, and E. Fleury: Surface silylation of cellulose microfibrils: preparation and rheological properties. *Polymer* **45,** 1569 (2004).
7. I.S. Goldstein: Cellulose: Nature and applications, in *Enclyclopedia of Materials Science and Engineering,* Vol. 1, edited by M.B. Bever (MIT Press, Cambridge, MA, 1986), p. 564.
8. R.H. Marchessault and P.R. Sundarrjan: In *Cellulose. The Polysaccharides*, Vol. 2, edited by G.O. Aspinall (Academic Press, New York, 1983), pp. 11–95.
9. A.C. O'Sullivan: Cellulose: The structure slowly unravels. *Cellulose* **4,** 173 (1997).
10. A.D. French: Structure and biosynthesis of cellulose. Part I: Structure, in *Discoveries in Plant Biology*, Vol. 3, edited by S.F. Yang and S.D. Kung (World Scientific, Singapore, 2000), pp. 163–197.
11. T. Ebeling, M. Paillet, R. Borsali, O. Diat, A. Dufresne, J-Y. Cavaillé, and H. Chanzy: Shear-induced orientation phenomena in suspensions of cellulose microcrystals, revealed by small angle x-ray scattering. *Langmuir* **15**(19), 6123 (1999).
12. L. Heux, G. Chauve, and C. Bonini: Nonflocculating and chiral -nematic self-ordering of cellulose microcrystals suspensions in nonpolar solvents. *Langmuir* **16,** 8210 (2000).
13. A. Dufresne, D. Dupeyre, and M.R. Vignon: Cellulose microfibrils from potato tuber cells: Processing and characterization of starch cellulose microfibril composites. *J. Appl. Polym. Sci.* **76,** 2080 (2000).
14. X.M. Dong, J-F. Revol, and D.G. Gray: Effect of microcrystallite preparation conditions on the formation of colloid crystals of cellulose. *Cellulose* **5,** 19 (1998).
15. M. Bercea and P. Navard: Shear dynamics of aqueous suspensions of cellulose whiskers. *Macromolecules* **33,** 6011 (2000).
16. X.M. Dong, T. Kimura, J-F. Revol, and D.G. Gray: Effects of ionic strength on the isotropic-chiral nematic phase transition of suspensions of cellulose crystallites. *Langmuir* **12,** 2076 (1996).
17. E. Dinand, H. Chanzy, and R.M. Vignon: Suspensions of cellulose microfibrils from sugar beet pulp. *Food Hydrocolloids* **13,** 275 (1999).
18. V. Favier, G.R. Canova, S.C. Shrivastava, and J.Y. Cavaillé: Mechanical percolation in cellulose whiskers nanocomposites. *Polym. Eng. Sci.* **37,** 1732 (1997).
19. P. Hajji, J.Y. Cavaillé, V. Favier, C. Gauthier, and G. Vigier: Tensile behavior of nanocomposites from latex and cellulose whiskers. *Polym. Compos.* **14,** 612 (1996).
20. V. Favier, H. Chanzy, and J.Y. Cavaillé: Polymer nanocomposites reinforced by cellulose whiskers. *Macromolecules* **28,** 6365 (1995).
21. A. Dufresne, J-I. Cavaillé, and W. Helbert: Thermoplastic nanocomposites filled with wheat straw cellulose whiskers. Part II: Effect of processing and modelling. *Polym. Compos.* **19**(2), 198 (1997).
22. A. Dufresne and M.R. Vignon: Improvement of starch film performances using cellulose microfibrils. *Macromolecules* **31,** 2693 (1998).
23. M.A.S. Azizi Samir, L. Chazeau, F. Alloin, J-Y. Cavaillé, A. Dufresne, and J-Y. Sánchez: POE-based nanocomposite polymer electrolytes reinforced with cellulose whiskers. *Electrochim. Acta* **50,** 3897 (2005).
24. M.A.S. Azizi Samir, F. Alloin, J-Y. Sanchez, and A. Dufresne: Cellulose nanocrystals reinforced poly(oxyethylene). *Polymer* **45,** 4149 (2004).
25. M.A.S. Azizi Samir, A. Montero Mateos, F. Alloin, J-Y. Sanchez, and A. Dufresne: Plasticized nanocomposite polymer electrolytes based on poly(oxyethylene) and cellulose whiskers. *Electrochim. Acta* **49,** 4667 (2004).
26. C. Goussé, H. Chanzy, G. Excoffier, L. Soubeyrand, and E. Fleury: Stable suspensions of partially silylated cellulose whiskers dispersed in organic solvents. *Polymer* **43,** 2645 (2002).
27. J. Urbanski: In *Handbook of Analysis of Synthetic Polymers and Plastics*, edited by J. Urbanski, W. Czerwinski, K. Janicka, F. Majewska, and H. Zowall (John Wiley & Sons, Poland, 1977), Chap. 1, pp. 48–53.
28. R.J. Young and P.A. Lovell: *Introduction to Polymers*, 2nd ed. (Chapman & Hall, London, UK, 1991).
29. N.E. Marcovich, M.M. Reboredo, and M.I. Aranguren: Modified woodflour as thermoset fillers. II Thermal degradation of woodflour and composites. *Termochimica Acta* **372,** 45 (2001).
30. S. Ardizzone, F.S. Dioguaardi, T. Mussini, P.R. Mussini, S. Rondinini, B. Verceli, and A. Vertova: Microcrystalline cellulose powders: Structure, surface features and water sorption capability. *Cellulose* **6,** 59 (1991).
31. H.P. Fink, E. Walenta, and J. Kunze: The structure of natural cellulose fibers—Part 2. The supermolecular structure of bast fibers and their changes by mercerization as revealed by x-ray diffraction and 13C-NMR spectroscopy. *Papier* **53,** 534 (1999).
32. M.N. Anglés and A. Dufresne: Platicized starch/tunicin whiskers

nanocomposites. 1. Structural analysis. *Macromolecules* **33,** 8344 (2000).
33. M.A.S. Azizi Samir, F. Alloin, J-Y. Sanchez, N. El Kissi, and A. Dufresne, Preparation of cellulose whiskers reinforced nanocomposites from an organic medium suspension. *Macromolecules* **37,** 1386 (2004).
34. N.E. Marcovich, M.M. Reboredo, J.M. Kenny, and M.I. Aranguren: Rheology of particle suspensions in viscoelastic media. Wood flour–polypropylene melt. *Rheologica Acta* **43,** 293 (2004).
35. M.I. Aranguren, E. Mora, J.V. DeGroot, Jr., and C.W. Macosko: Effect of reinforcing fillers on the rheology of polymer melts. *J. Rheol.* **36,** 1165 (1992).
36. E. Guth: Theory of filler reinforcement. *J. Appl. Phys.* **16,** 20 (1945).
37. I.M. Krieger: Rheology of monodisperse latices. *Adv. Colloid Interface Sci.* **3,** 111 (1972).
38. A.B. Metzner: Rheology of suspensions in polymeric liquids. *J. Rheol.* **29,** 739 (1985).
39. A.R. Payne and R.E. Whittaker: Effect of vulcanization on the low-strain dynamic properties of filled rubbers. *J. Appl. Polym. Sci.* **16,** 1191 (1972).
40. R. Kotsilkova, D. Nesheva, I. Nedkov, E. Krusteva, and S. Stavrev: Rheological, electrical, and microwave properties of polymers with nanosized carbon particles. *J. Appl. Polym. Sci.* **92,** 2220 (2004).
41. F. Du, R.C. Scogna, W. Zhou, S. Brand, J.E. Fisher, and K.I. Winey: Nanotube networks in polymer nanocomposites: Rheology and electrical conductivity. *Macromolecules* **37,** 9048 (2004).
42. O. Meincke, D. Kaempfer, H. Weickmann, C. Friedrich, M. Vathauer, and H. Warth: Mechanical properties and electrical conductivity of carbon-nanotube filled polyamide-6 and its blends with acrylonitrile/butadiene/styrene. *Polymer* **45,** 739 (2004).
43. J. Mewis and C.W. Macosko: In *Rheology. Principles, Measurements, and Applications* (VCH Publishers, New York, 1994), Chap. 10.
44. L.A. Hough, M.F. Islam, P.A. Janmey, and A.G. Yohd: Viscoelasticity of single wall carbon nanotube suspensions. *Phys. Rev. Lett.* **93,** 168102 (2004).
45. A. Dani and A.A. Ogale: Electrical percolation behavior of short-fiber composites: Experimental characterization and modeling. *Compos. Sci. Technol.* **57,** 1355 (1997).
46. W.J. Cantwell and A.C. Roulin-Moloney: In *Fractography and Failure Mechanisms of Polymers and Composites*, edited by A.C. Roulin-Moloney (Elsevier Applied Sicence, London, UK, 1989), Chap. 7, pp. 256–258.
47. W.J. Cantwell, A.C. Roulin-Moloney, and T. Kaiser: Fractography of unfilled and particulate-filled epoxy resins. *J. Mater. Sci.* **23,** 1615 (1988).
48. S. Bandyopadhyay: Review of the microscopic and macroscopic aspects of fracture of unmodified epoxy resins. *Mater. Sci. Eng. A* **125,** 157 (1990).
49. H.H. Kausch: *Polymer Fracture,* 2nd ed. (Springer Verlag, Germany, 1987), Chap. 9, p. 382.
50. B. Cotterell: Facture propagation in organic glasses. *Int. J. Fract. Mech.* **4,** 209 (1968).
51. N.E. Marcovich, M.I. Aranguren, and M.M. Reboredo: Modified woodflour as thermoset fillers. I. Effect of the chemical modification and percentage of filler on the mechanical properties. *Polymer* **42,** 815 (2001).
52. A.J. Nuñez, P.C. Sturm, J.M. Kenny, M.I. Aranguren, N.E. Marcovich, and M.M. Reboredo: Mechanical characterization of PP-woodflour composites. *J. Appl. Polym. Sci.* **88,** 1420 (2003).
53. X. Kornmann, L.A. Berglund, J. Sterte, and E.P. Giannelis: Nanocomposites based on montmorillonite and unsaturated polyester. *Polym. Eng. Sci.* **38,** 1351 (1998).
54. W. Helbert, J.Y. Cavaillé, and A. Dufresne: Thermoplastic nanocomposites filled with wheat straw cellulose whiskers. Part I: Processing and mechanical behavior. *Polym. Compos.* **17,** 604 (1996).
55. Y. Bréchet, J.Y. Cavaillé, E. Chabert, L. Chazeau, R. Dendievel, L. Flandin, and C. Gauthier: Polymer based nanocomposites: Effect of filler-filler and filler-matrix interactions. *Adv. Eng. Mater.* **3,** 571 (2001).